Fat-saturated Diffusion-weighted Imaging of the Rat Pelvis using Three-Dimensional MP-RAGE MR sequence

T. Numano, K. Homma, N. Iwasaki, K.Hyodo, and N. Nitta

Abstract— **In this work we report on the development of a novel technique for fat-saturated three-dimensional (3D) diffusion-weighted (DW) MRI sequence based upon 3D magnetization-prepared rapid gradient-echo (3D-MP-RAGE). In order to saturate fat, two kinds of procedures were competed CHESS-DW-3D-MP-RAGE sequence (CHESS -3D-DWI) and DW-3D-MP-WE-RAGE sequence (WE-3D-DWI) "chemical shift selective: CHESS method vs. water-excitation: WE method". The CHESS-3D-DWI sequence and WE-3D-DWI sequence were compared in terms of their degree of fat suppression. In CHESS-3D-DWI sequence a preparation phase with a "CHESS-90°RF-motion probing gradient: MPG-180°RF -MPG-90°RF" pulse-train was used to sensitize the magnetization to fat-saturated diffusion. In contrast, WE-3D-DWI sequence a RAGE-excitation pulse with a "binominal -pulse 1-1 or 1-2-1" was selected to water-excited (fat-saturated) diffusion imaging. These imaging were done during in vivo studies using an animal experiment. From experimental results obtained with a phantom, the effect of diffusion weighting and the effect of fat-saturation were confirmed. Fat-saturation was much better in the WE-3D-DWI sequence than CHESS-3D-DWI sequence. From rat experimental results, fat-saturated diffusion-weighted image data were obtained. This sequence was useful for in vivo imaging.**

I. Introduction

The utility of diffusion-weighted magnetic resonance imaging (DWI) for the diagnosis of acute cerebral infarction has now thoroughly established [1,2]. At the same time, diffusion tensor imaging (DTI) has emerged as a widely used quantitative magnetic resonance technique for the investigation of structural and orientational changes in brain tissue during development and in pathological states in vivo [3,4]. In recent years, a DWI is just beginning to be applied to body diffusion weighted imaging (body-DWI) [5,6].

The implementation of single-shot (SS) echo-planar imaging (EPI) with diffusion weighting has been very effective in reducing the time taken to acquire a set of diffusion-weighted (DW) images. However, SS-DW-EPI, like all EPI acquisition in general, has a notoriously high level of artifacts. The classic EPI artifact is the N/2 (Nyquist) ghost. This arises because of imperfections in the rephrasing-dephasing cycle of the rapidly switching bipolar frequency-encode gradient. Another artifact is a consequence of bandwidth. Each frequency-encode lobe is sampled 64 or 128 times over the whole gradient-echo train. This rather slow sampling rate means that the signal bandwidth in the phase-encode direction may be as little as 10Hz/pixel. This gives magnetic field differences, e.g., in the vicinity of air-tissue interface, which will result in large signal alterations and geometric distortions. Furthermore, a large measure of SS-DW-EPI is two-dimensional (2D) multislice imaging. In order to perform multislice imaging, it is necessary to have a few millimeters of slice thickness and slice gap. 2D multislice imaging has limited imaging resolution in the slice-selection direction, which may inhibit the study of small structures. Thus, the author goes on to develop an alternative three- dimensional (3D) magnetization -prepared rapid gradient- echo (3D-MP-RAGE) MRI sequence which allows for rapid mapping of diffusion properties without sensitivities to tissue susceptibility differences, magnetic field inhomogeneities [7,8].

Parallel imaging techniques like sensitivity encoding (SENSE) greatly enhances the quality of SS-DW-EPI by reducing blurring and off-resonance artifacts. In consequence, SS-DW-EPI began to be used also for the body-DWI. This strategy is similar to positron emission tomography (PET) imaging. However, it is difficult to obtain PET-like images because insufficient fat suppression. Therefore, when applying a diffusion weighted image method to the body section, concomitant use of an exact fat-suppression method is needed for. In order to attain the fat-saturated three-dimensional diffusion weighted imaging, we developed two kinds of procedures were competed "chemical shift selective: CHESS method [9] vs. water -excitation: WE method [10,11]" CHESS-DW-3D -MP-RAGE sequence (CHESS-3D-DWI) and DW-3D-MP -WE-RAGE sequence (WE-3D-DWI). In this paper, we investigate the potential of the fat-saturated 3D- MP-RAGE sequences for diffusion-weighted 3D imaging.

II. Material and Methods

A. Three-dimensional DWI sequence

Fig. 1 shows the base module (3D-DWI) sequence. This method combines the DW driven equilibrium Fourier transform (DW-DEFT) preparation with a 3D-MP-RAGE imaging module. In this sequence, the preparation phase with

Manuscript submitted April 1, 2007. This work was supported in part by the Grant-in-Aid for Scientific Research (15591084, 18790902).

Tomokazu NUMANO: Dept. of Radiological Science, Tokyo Metropolitan University, Tokyo, Japan (corresponding author to provide phone: +81-3-3819-1211; fax: +81-3-3819-1406; e-mail: t-numano@ post.metro-hs.ac.jp).

K. Homma, K. Hyodo, and N. Nitta: Biomedical Sensing and Imaging Group, National Institute of Advanced Industrial Science and Technology (AIST), Tsukuba, Japan.

N. Iwasaki: Dept. of Pediatrics, Ibaraki Prefectural University of Health Sciences, Ibaraki, Japan.

"90^{o}_{x}RF- motion proving gradient: MPG- 180^{o}_{y}RF- MPG- 90^{o}_{-x}RF" pulse train (DW-DEFT) was used to sensitize the magnetization to diffusion. A centric k-space acquisition ordered RAGE-loop sequence was necessary to minimize saturation effects from tissues with short relaxation times. For further details, see Ref. [7]. Adding improvements to this sequence developed the CHESS-3D-DWI sequence, and the WE-3D-DWI sequence.

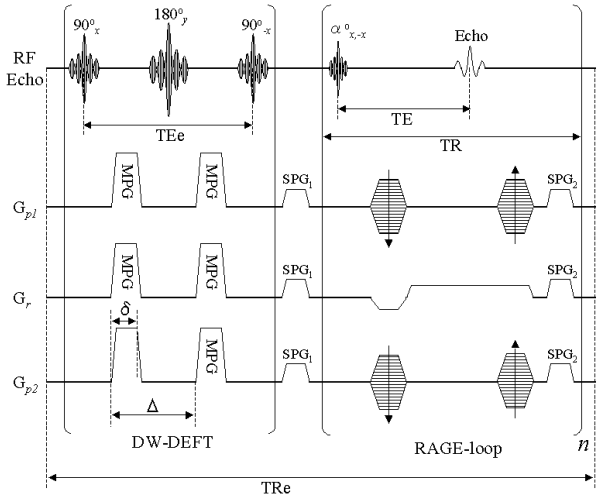

Fig. 1. Diagram of the 3D MP-RAGE MRI pulse sequence used for 3D diffusion mapping (3D-DWI). The slice phase-encode gradient (G_{p1}-PEG) happens only once per TRe period. On the other hand, the phase-encode gradient (G_{p2}-PEG) changed in each TR period. In order to avoid T1-contamination in the DW image, the phase encoding was centric k-space acquisition order.

B. Chemical shift selective 3D-DWI (CHESS-3D-DWI) sequence

Fig. 2 shows the chemical shift selective 3D-DWI (CHESS-3D-DWI) sequence. This method combines the CHESS pulse with a 3D-DWI sequence. In order to suppress the fat signal by the saturation bandwidth of 300 Hz, the CHESS pulse was set as 19ms of the sinc wave. The signal of oil (fat) phantom was most saturated, when the offset frequency of a CHESS pulse was 250Hz.

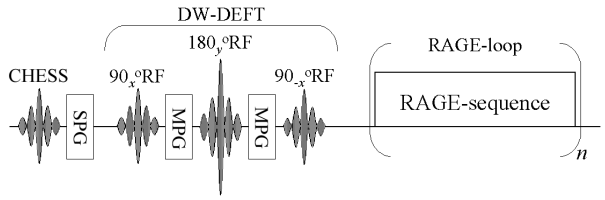

Fig. 2. Diagram of the 3D-DWI pulse sequence used for fat-sarurated diffusion mapping (CHESS-3D-DWI). In order to suppress the fat signal, the CHESS-3D-DWI sequence was made from extending a CHESS pulse to the 3D-DWI.

C. Water-excitation 3D-DWI (WE-3D-DWI) sequence

Fig. 3 shows the water-excitation 3D-DWI (WE-3D-DWI) sequence. In order to achieve a water-excitation (fat-saturation) effect, we chose a binominal pulse as the excitation pulse of RAGE sequence. The effect of water-excitation (fat-saturation) was experimentally verified by two kinds of binominal series, i.e. 1:1, and 1:2:1.

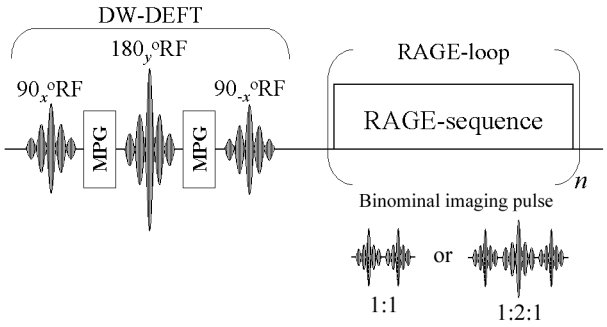

Fig. 3. Diagram of the 3D-DWI pulse sequence used for water-excited (fat-saturated) diffusion mapping (WE-3D-DWI). In order to suppress the fat signal, the WE-3D-DWI sequence was made from exchange a binominal imaging pulse in the 3D-DWI.

D. Phantom experiment: Comparison of CHESS-3D-DWI vs. WE-3D-DWI

All MRI experiments were performed on a 2.0-T Biospec 20/30 System with a B-GA20 Gradient System (Bruker, Karlsruhe, Germany) that had a maximum gradient strength of 100mT/m. The MR data acquisition and reconstruction were performed with the ParaVision (Bruker) software system. A 72-mm-ID birdcage coil tuned to 85 MHz for proton resonance was used for all measurements. The phantom was made of a series of 1.65-cm-diameter tubes containing cooking oil, and containing various concentration of acetone. The concentration of acetone varied from 0% (water phantom) to 100% (acetone phantom), with a step size of 20%. All phantom experiments were performed at room temperature at 23°C.

The parameters of base module (3D-DWI) sequence were 10000 ms/30.74 ms (effective-TR: TRe/ effective-TE: TEe), 8.91ms/4.7ms (TR/TE), FA of 35°, readout bandwidth of 390Hz/pixel, matrix of 128x128x8, field of view (FOV) of 70x70x80 mm, 128 phase-encoding step per RAGE loop, MPG duration (δ) of 13.00ms, MPG separation (Δ) of 15.37ms, MPG-power varied from 0 to 90mT/m (b-value: 0, 68, 270, 608, 1081s/mm^2), MPGs were applied to all direction. The CHESS-3D-DWI sequence was made from extending a CHESS pulse to this base module. The WE-3D-DWI sequence was made from exchange a binominal imaging pulse in this base module. The total acquisition time of both of the pulse sequences was 6min 41s.

E. Animal experiment

To evaluate in vivo application of the WE[1:2:1]-3D-DWI sequence, we experimented on a rat. The female Crj:Wistar rat was anesthetized by intraperitoneal injection of ketamine (100mg/kg body weight), xylazine (10mg/kg body weight) and atropine (0.05mg). The maintenance of anesthesia was controlled by inhalation of halothane (0.75%) from an inhalation anesthesia apparatus. The WE-3D-DWI sequence parameters were 3000 ms/54.74 ms (TRe/ TEe), 8.91 ms/4.7 ms (TR/TE), FA of 35°, readout bandwidth of 195 Hz/pixel,

matrix of 64x64x64, FOV of 70x70x70, 64 phase-encoding step per RAGE loop, MPG duration (δ) of 25.00 ms, MPG separation (Δ) 27.37 ms, MPG-power varied from 0 to 30mT/m (b-value: 0, 1000s/mm^2), MPGs were applied to readout direction. The total acquisition time was 13 min 3s. This animal experiment was performed in accordance with animal protection laws and approved by the Animal Ethical Committee of the National Institute of Advanced Industrial Science and Technology.

III. Results

A. Phantom experiments

Fig. 4 shows selected fat-saturated phantom images (3D-DWI, CHESS-3D-DWI, WE[1:1]-3D-DWI, and WE [1:2:1]-3D-DWI) and corresponding water phantom images. The white lines across the images show the locations in which the signal profiles were obtained. The solid line is water phantom, and the dash line is oil phantom. Compared with 3D-DWI sequence without a fat saturation effect, CHESS -3D-DWI sequence and WE-3D-DWI sequence have saturated the signal from an oil phantom. Compared with CHESS-3D-DWI sequence, WE-3D-DWI sequence has saturated the signal from an oil phantom without the edge enhancement effect.

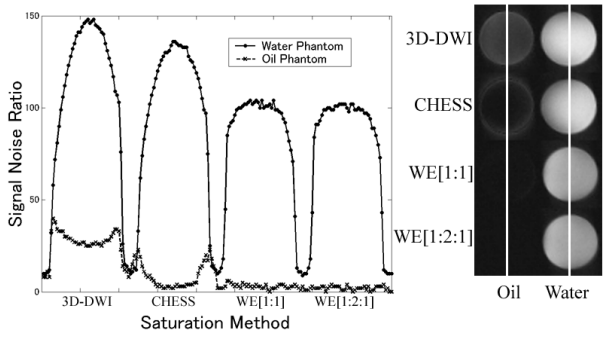

Fig. 4. Phantom experiment results with different fat-saturation method for the water/oil phantoms. The solid line is water phantom, and the dash line is oil phantom.

As for the result of the diffusion coefficient comparative experiments using various concentration acetone phantoms, the almost equivalent result was obtained (data is not shown).

B. Animal experiment

Fig. 5A-D illustrates rat pelvis 3D imaging results recorded by the 3D-DWI sequence (A,B), and the WE[1:2:1]-3D-DWI sequence (C,D). These images were obtained with *b* values of 0 (A,C), 1000 (B,D) s/mm^2. In these images, the effect of increasing the MPG strength was seen as a decrease in image intensity. Fig. 6 shows selected diffusion-weighted axial (arbitrary section: axial image) images (0, 1000 s/mm^2) and the corresponding parametric image of the calculated apparent diffusion coefficient map. When the 3D-DWI axial image (A) and the WE[1:2:1]-3D-DWI axial image (D) were compared, the fatty tissue of the WE[1:2:1]-3D-DWI axial image was saturated by water excitation effect. Additionally, the chemical shift artifact in the vesica urinaria surrounded by fatty tissue has not generated by the water excitation effect. In the ADC-maps, the calculated apparent diffusion coefficients (3D-DWI sequence / WE[1:2:1]-3D-DWI sequence) of vesica urinaria and muscle were 1.33/ 2.29 [x10^{-3} mm^2/s] and 0.84/ 1.89 [x10^{-3} mm^2/s], respectively.

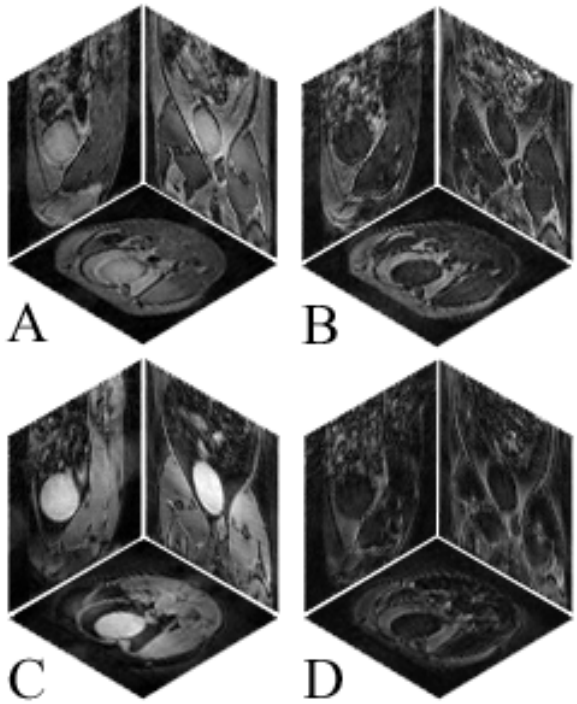

Fig. 5. Three-dimensional rat pelvis diffusion-weighted MR images obtained with *b* value of 0 (A,C) 1000 (B,D) s/mm^2. In these images, the effect of increasing the MPG strength was seen as a decrease in image intensity.

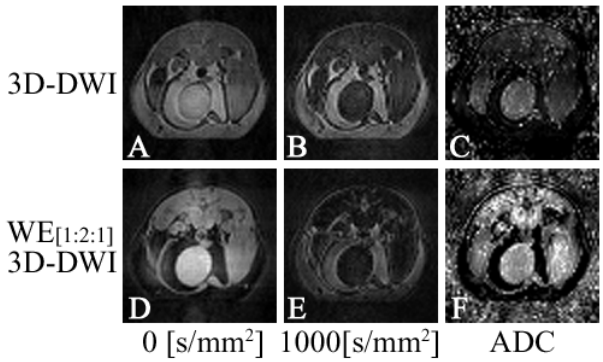

Fig. 6. The 3D-DWI axial image (top row) and the WE[1:2:1] -3D-DWI axial image (bottom row) of rat pelvis. The fatty tissue of the WE[1:2:1]-3D-DWI image was saturated by water excitation effect.

IV. Discussion

Diffusion-weighted magnetic resonance imaging (DWI) has become an important component of the modern imaging armamentarium for the diagnosis of acute cerebral infarction. In recent years, MRI scanners have become increasingly

sophisticated, and DWI extended the territory of activity further. One of the important advancements in the recent DWI is measurement of incoherent directional distribution of diffusivity, that is anisotropy, for application of visualizing white matter fiber tracts, and the technique has been developed to diffusion tensor imaging (DTI). On another recent DWI front, recent advances in MR gradient technology allow acquisition of DWI with high *b* value even in the body, thanks to the advent of fast imaging sequence like EPI and parallel imaging techniques like SENSE. However, since trunk of the body has much fatty tissue, body-DWI sequence needs to incorporate an accurate fat-saturation method. In this paper, a newly developed the fat-saturated 3D-MP-RAGE sequence for diffusion-weighted 3D imaging was successfully applied to in vivo rat pelvis.

The CHESS-3D-DWI sequence and the WE-3D-DWI sequence were able to saturation the signal from oil-phantom, but the edge enhancement effect of a fat phantom was looked at by the fat-saturated effect by the CHESS-3D-DWI sequence. Fig. 7 shows the collected echo peaks (only the readout gradient was applied, and only one-direction FT^{-1}) vs. one-time (one TRe loop) rapid gradient echo acquisitions.

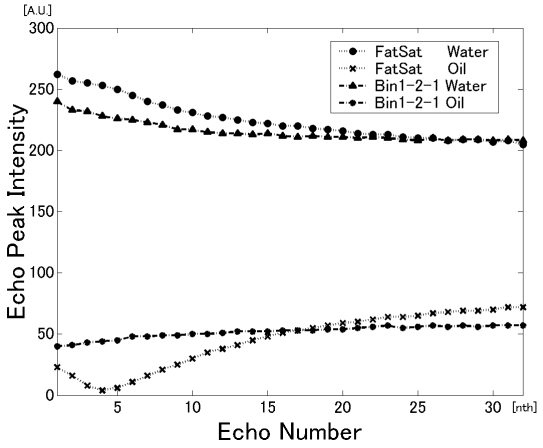

Fig. 7. Collected echo peaks (the first 32 echoes of shooting) versus RAGE-loops (only the readout gradient was applied) of the CHESS-3D-DWI sequence and the WE[1:2:1]-3D-DWI sequence.

When the phase encoding (RAGE-loop) is set to 128 steps, 128 echoes queue up. In the Fig. 7, in order to make it clear, the peak value from the start to the 32nd was displayed. When the number of times of RAGE-loop increases, as opposed to the peak value of a water phantom shifting to a steady state, the peak value of a fat phantom by the CHESS-3D-DWI was gradual climb. Since it depends for change of a peak value on T1 of water or fat, even if the CHESS pulse saturated the magnetization, fat magnetization with short T1 is recovered in the duration of RAGE-loop. As a result, since the *k*-space acquisition order of base module (3D-DWI) sequence was centric, although the fat-saturation effect is effective against the low-frequency component signal from the fat phantom, the high-frequency component signal from the fat phantom is not saturated. In other words, it becomes a meaning equivalent to the status that k-space filtering. In contrast, since WE-3D-DWI sequence always excites water, the signal from a fat phantom is always saturated. Since the edge enhancement effect of a fat phantom dose not occurs, the WE-3D-DWI sequence is a useful procedure compared with CHESS -3D-DWI sequence.

V. Conclusion

In conclusion, a new fat-saturated diffusion weighted three-dimensional MR sequences were developed and discussed. From the results of phantom experiments, since WE-3D-DWI does not cause the edge enhancement effect, it had the performance exceeding CHESS-3D-DWI sequence. From the result of rat pelvis experiments, the WE[1:2:1]-3D-DWI sequence will provide useful information for clinical diagnosis.

References

[1] ME. Moseley, Y. Cohen, J. Mintorovitch, L. Chileuitt, H. Shimizu, J. Kucharczyk, MF. Wendland, PR. Weinstein, "Early detection of regional cerebral ischemia in cats: comparison of diffusion- and T2-weighted MRI and spectroscopy," *Magn Reson Med*, vol. 14(2), pp. 330-46, May 1990.

[2] BJ. Dardzinski, CH. Sotak, M. Fisher, Y. Hasegawa, L. Li, K. Minematsu, "Apparent diffusion coefficient mapping of experimental focal cerebral ischemia using diffusion-weighted echo-planar imaging," *Magn Reson Med*, vol. 30(3), pp. 318-25, Sep 1993.

[3] PJ. Basser, J. Mattiello, D. LeBihan, "Estimation of the effective self-diffusion tensor from the NMR spin echo," *J Magn Reson B,* vol. 103(3), pp.247-54, Mar 1994.

[4] C. Pierpaoli, P. Jezzard, PJ. Basser, A. Barnett, G. DiChiro, "Diffusion tensor MR imaging of the human brain," *Radiology*, vol. 201(3), pp. 637-48, Dec 1996.

[5] T. Kinoshita, N. Yashiro, N. Ihara, H. Funatu, E. Fukuma, M. Narita, "Diffusion-weighted half-Fourier single-shot turbo spin echo imaging in breast tumors: differentiation of invasive ductal carcinoma from fibroadenoma," *J Comput Assist Tomogr*, vol. 26(6), pp. 1042-6, Nov-Dec 2002.

[6] T. Takahara, Y. Imai, T. Yamashita, S. Yasuda, S. Nasu, MV. Cauteren, "Diffusion weighted whole body imaging with background body signal suppression (DWIBS): technical improvement using free breathing, STIR and high resolution 3D display," *Radiat Med*, vol. 22(4), pp. 275-82, Jul-Aug 2004.

[7] T. Numano, K. Homma, T. Hirose. "Diffusion-weighted three-dimensional MP-RAGE MR imaging," *Magn Reson Imaging*, vol. 23(3), pp. 463-8, Apr 2005.

[8] T. Numano, K. Homma, N. Iwasaki, K. Hyodo, N. Nitta, T. Hirose. "In vivo isotropic 3D diffusion tensor mapping of the rat brain using diffusion-weighted 3D MP-RAGE MRI," *Magn Reson Imaging*, vol. 24(3), pp. 287-93, Apr 2006.

[9] J. Frahm, A. Haase, W Hanicke, D. Matthaei, H. Bomsdorf, T. Helzel. "Chemical shift selective MR imaging using a whole-body magnet," Radiology, vol. 156(2), pp. 441-4, Aug 1985.

[10] GC. Clore, BJ. Kimber, AM. Gronenborn, "The 1-1 Hard Pulse: A Simple and Effective Method of Water Resonance Suppression in FT ^{1}H NMR," *J Magn Reson*, vol. 54, pp. 170-3, 1983.

[11] V. Sklenar, Z. Starcuk. "1-2-1 Pulse Train: A New Effective Method of Selective Excitation for Proton NMR in Water," *J Magn Reson*, vol. 50, pp. 495-501, 1982.